Electronic Supplementary Material (ESI) for Journal of Materials Chemistry C.

Supplementary information

Improved performance of planar perovskite devices via inclusion of ammonium acid iodide (AAI) derivatives using two step inter-diffusion process

Neeti Tripathi,[a]* Masatoshi Yanagida,[b] Yasuhiro Shirai,[b]* Kenjiro Miyano[b]

[a]*Department of Physics, School of Physical Sciences (SoPS), Doon University, Dehradun 248001, Uttarakhand, INDIA*

[b]*Global Research Center for Environment and Energy based on Nanomaterials Science (GREEN), National Institute of Materials Science (NIMS), 1-1 Namiki, Tsukuba, Ibaraki 305-0044, JAPAN.*

Email: neetidtripathi@gmail.com, SHIRAI.Yasuhiro@nims.go.jp

Experimental:

All chemicals were purchased from commercial suppliers and used as received, unless stated otherwise. Perovskite precursor solutions were prepared by dissolving PbI_2 [Sigma-Aldrich, 99% purity] and methylammonium iodide (MAI) [Wako Chemicals] in anhydrous dimethylformamide (400 mg mL^{-1}) and ethanol (50 mg mL^{-1}), respectively. Additives $C_2H_6INO_2$, $C_4H_{10}INO_2$, and $C_6H_{14}INO_2$ were synthesised from respective amino acids derivatives [Wako Chemicals]. These amino acid derivatives were reacted with hydroiodic acid (~ 2 eq.) in H_2O at 0 °C for ~ 3 hours, and respective products were isolated after the removal of solvent then washing with ethanol. To prepare the additive solution, these additives were mixed in the PbI_2 solution (5 gm mL^{-1}) and stirrer at 70 °C overnight to make the homogenous additive solution. $PC_{61}BM$ [Solenne, 99% purity] solution (2 wt %) dissolved in anhydrous CB was used for coating of the electron transport layer. A thin layer of (poly[9,9-bis(3′-(N,N-dimethylamino)- propyl)-2,7-fluorene)-alt-2,7-(9,9-dioctylfluorene)] PFN [1-Material] was used for interfacial engineering by using the solution in anhydrous ethanol (2 mg in 16 mL^{-1}). All solutions were filtered through 0.45 μm syringe filters to avoid the risk of particle formation. Time-of-flight secondary ion mass spectrometry (TOF-SIMS) analysis was performed with a TOFSIMS5 (ION-TOF GmbH) instrument. TOF-SIMS depth profiles from detection of positive secondary ions were acquired by using a pulsed 60 kV $Bi_3{}^{2+}$ for analysis and 5 kV or 10 kV $Ar_{2000}{}^{+}$ gas cluster ion beams for sputtering. The sputtered area was 300 × 300 μm and the analysis area was 100 × 100 μm. Depth profiles were obtained with the noninterlaced mode of sputtering/analysis cycles. The X-ray diffraction patterns were collected by using a Bruker D8 advanced. Cross-sectional images were taken under a high-resolution scanning electron microscope (Hitachi-4800) at a 5 kV accelerating voltage carefully to avoid damages to the samples. The current density− voltage (J−V) characteristics and incident monochromatic IPCE spectra or external quantum efficiency (EQE) were measured with a CEP-200BX spectrometer (Bunkokeiki, Tokyo, Japan). For photostability testing, the device was evaluated under short-circuit and open-circuit conditions continuously for 20 min time intervals under continuous illumination (1 sun). To investigate hysteresis behavior, scan rates were varied from 0.02 to 0.4 V/s. A histogram of 15 devices were deduced from the active device area of 0.18 cm^2 defined by an aperture mask.

Device Fabrication:

Solar cell devices were fabricated on pre-cleaned patterned indium tin oxide (ITO)-coated glass substrates (15 Ω $square^{-1}$). The ITO substrates were pre-cleaned in an ultrasonic bath with detergent, pure water, and 2-propanol, followed by ultraviolet-ozone treatment for 5 min to remove organic residuals. A thin layer (30 nm) of PEDOT:PSS (Clevios, Al4083) was formed by spin coating at 3000 rpm and subsequently dried at 140 °C for 10 min on a hot plate under ambient conditions. Substrates were transferred to a nitrogen-filled glovebox (<1.0 ppm of O_2 and H_2O), inside which the rest of the steps were performed. To carry the perovskite film formation using two step deposition method, first 40 wt% of PbI_2 solution in N,N-Dimethylmethanamide (DMF) was then spin coated at 3000 rpm for 35 s and subsequently dried at 70 °C for 30 min. After that, a mixed solution of (MAI + MACl) (95+5) mg/2 ml in ethanol was then spun on to the PbI_2 layer at 4000 rpm for 35 s. The film was then further annealed at 100°C for 2 h to promote crystallization of the $CH_3NH_3PbI_xCl_{3-x}$ perovskite. For the formation of additive mixed perovskite film, $C_2H_6INO_2$, $C_4H_{10}INO_2$, and $C_6H_{14}INO_2$ were mixed in the PbI_2 solution (5 mg/ml), followed by the coating of MAI + MACl solution, similar to the procedure opted for the pure perovskite film. A $PC_{61}BM$ layer was spun-cast onto the perovskite layer at 700 rpm for 60 s, and this was followed by coating with the PFN-P2 layer at 3000 rpm for 50 s. Samples were then transferred to the evaporation chamber connected to the glovebox for metal contact deposition. Finally, 100 nm of Ag was thermally evaporated at a pressure $<10^{-4}$ Pa. Devices were sealed by using UV curable resins (UV RESIN XNR5516Z, Nagase ChemteX, Japan) before measurement under ambient conditions, and electrical connections were made through the ITO patterns. For the long term stability testing, encapsulated devices were stored at ambient conditions.

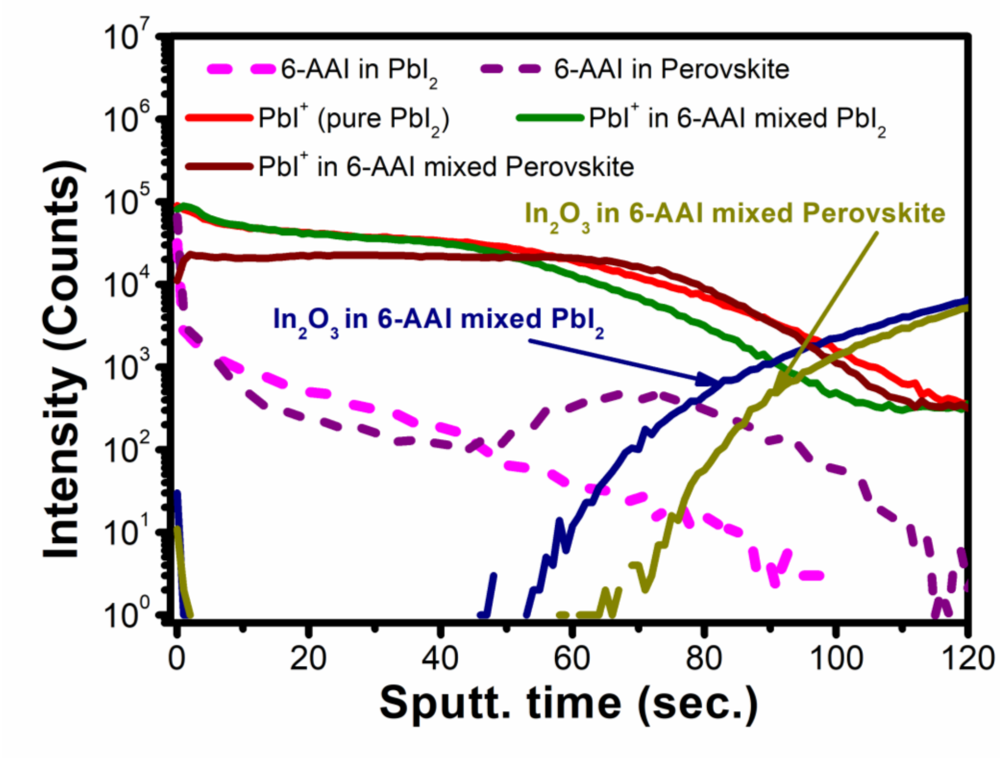

Figure S1: TOF-SIMS graph for 6-AAI mixed PbI_2, pure perovskite and 6-AAI mixed perovskite films.

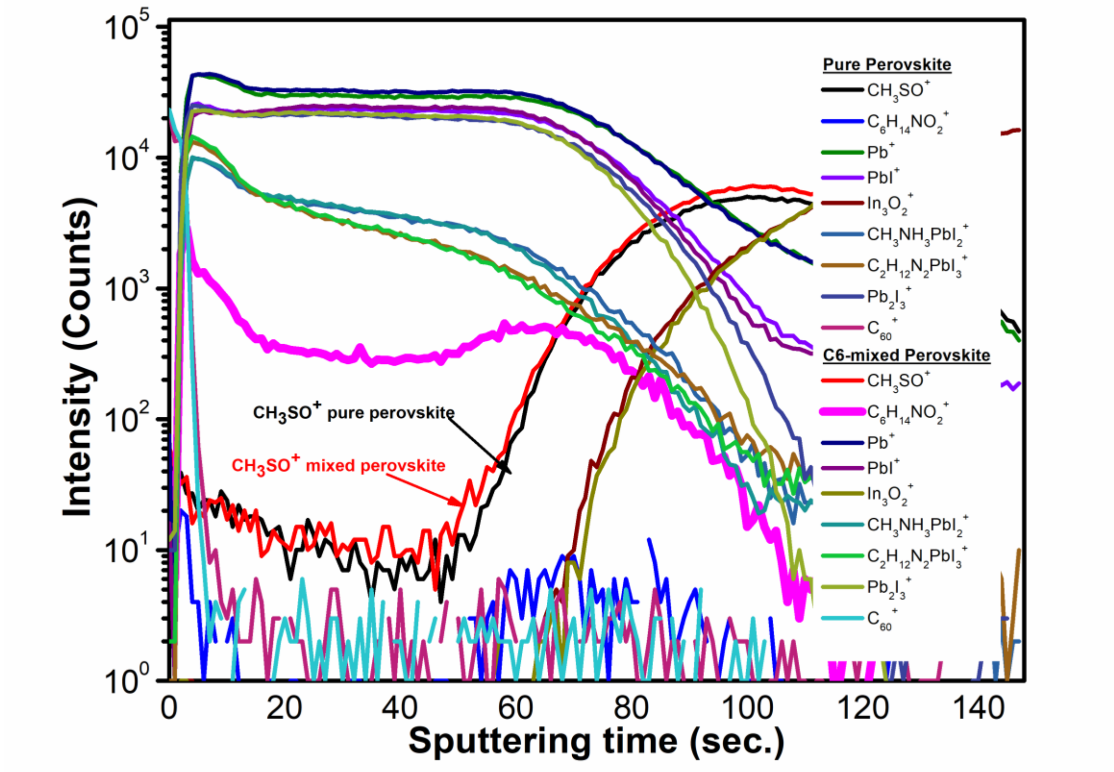

Figure S2: TOF-SIMS graph for pure and 6-AAI mixed perovskite films for thickness comparison.

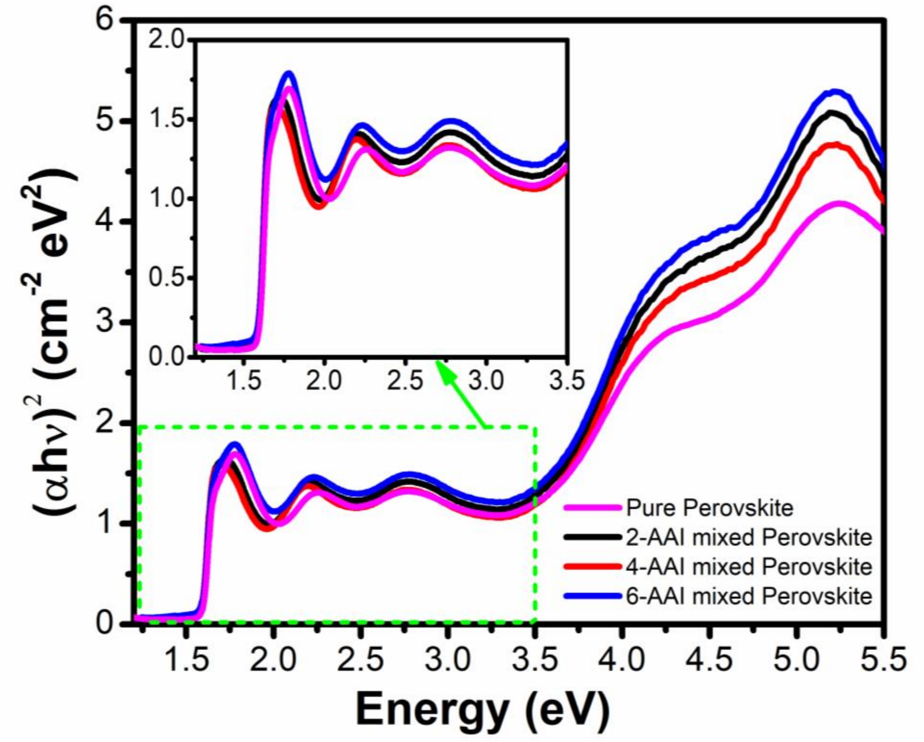

Figure S3: UV-visible absorbance spectra for pure and AAI-mixed perovskite films.

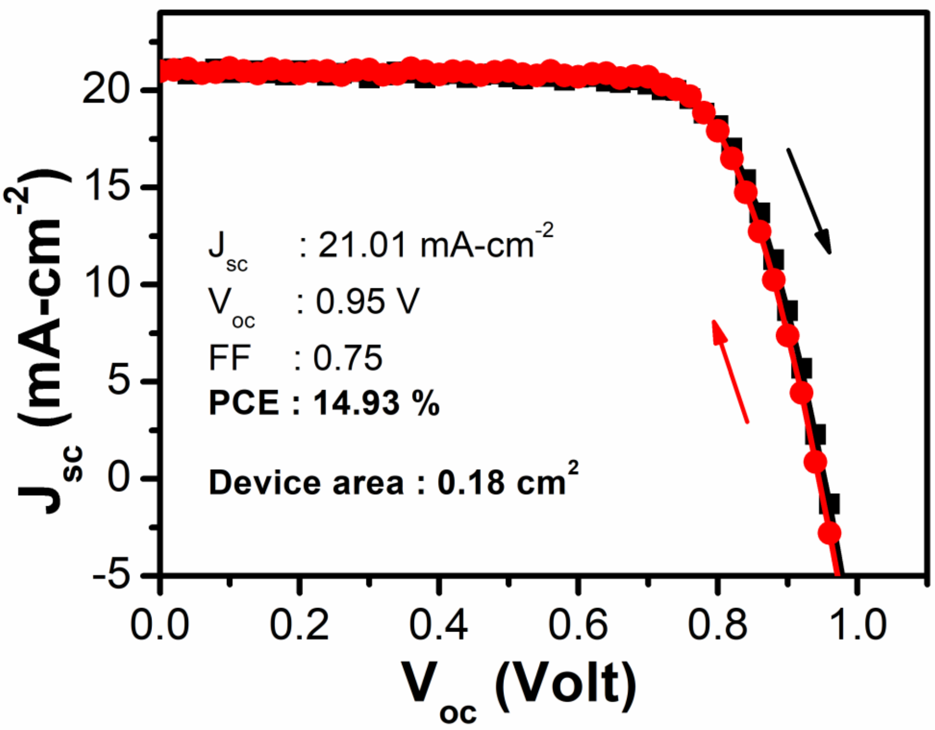

Figure S4: J-V characteristics of the champion device with active device area 0.18 cm^2.

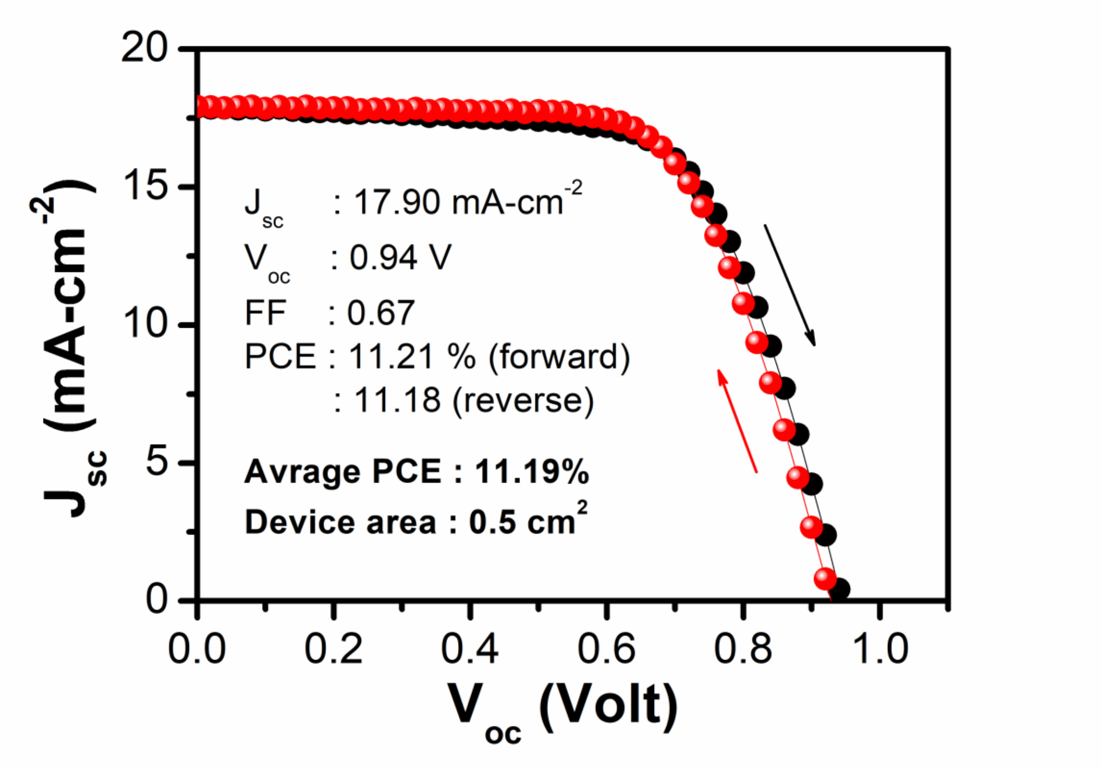

Figure S5: J-V characteristics of the 6-AAI mixed perovskite solar device with active device area 0.5 cm^2.

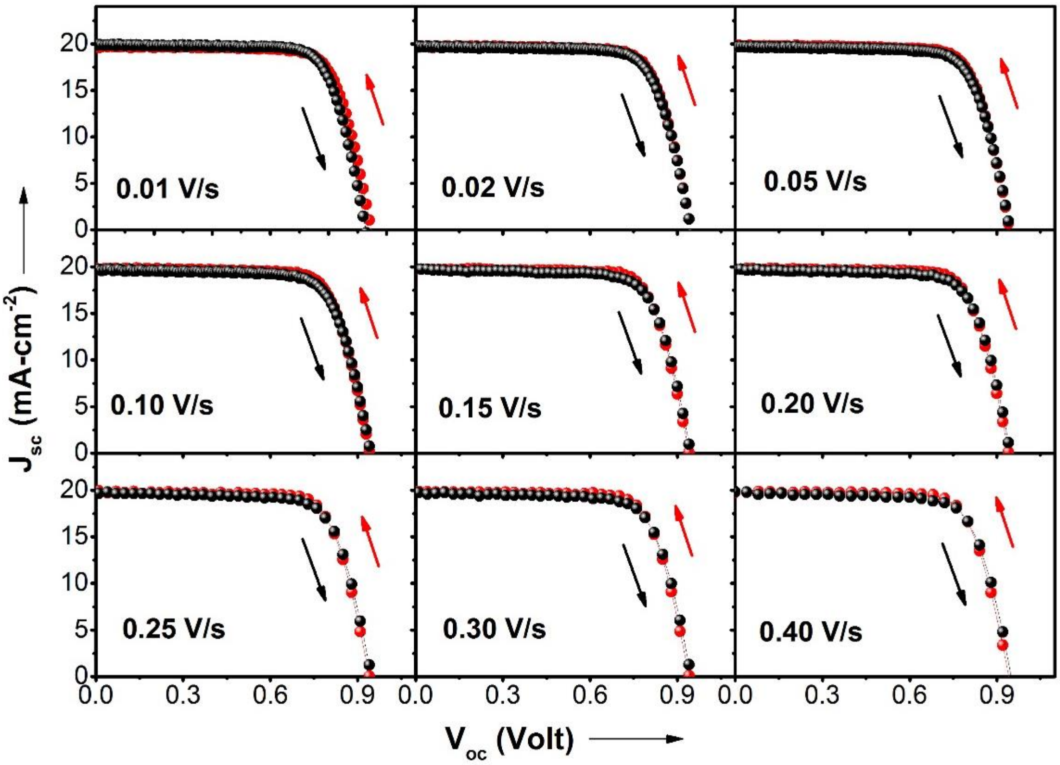

Figure S6: J-V characteristics of 6-AAI mixed perovskite device (active device area 0.18 cm^2) at various scan rates.

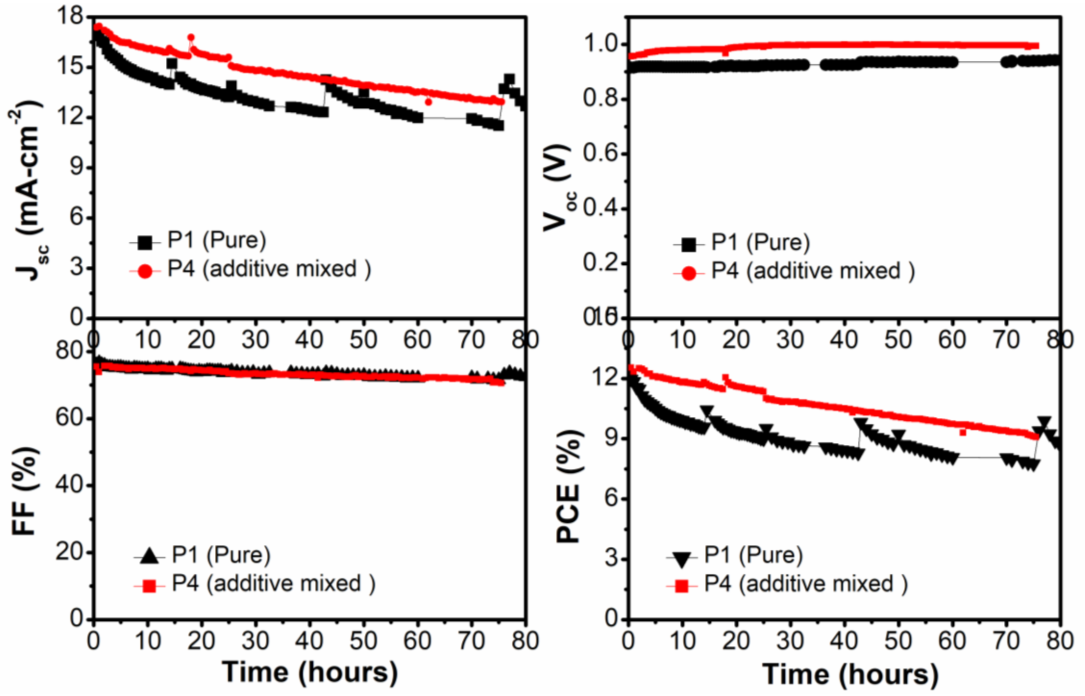

Figure S7: Durability test of pure and 6-AAI mixed perovskite device.

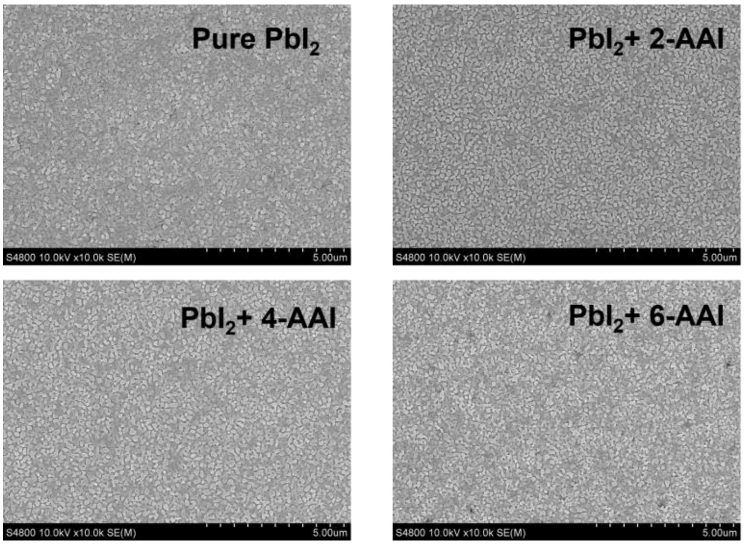

Fig. S8: Low magnification SEM images of Pure PbI_2, PbI_2 + 2AAI, PbI_2 + 4AAI, and PbI_2 + 6-AAI.

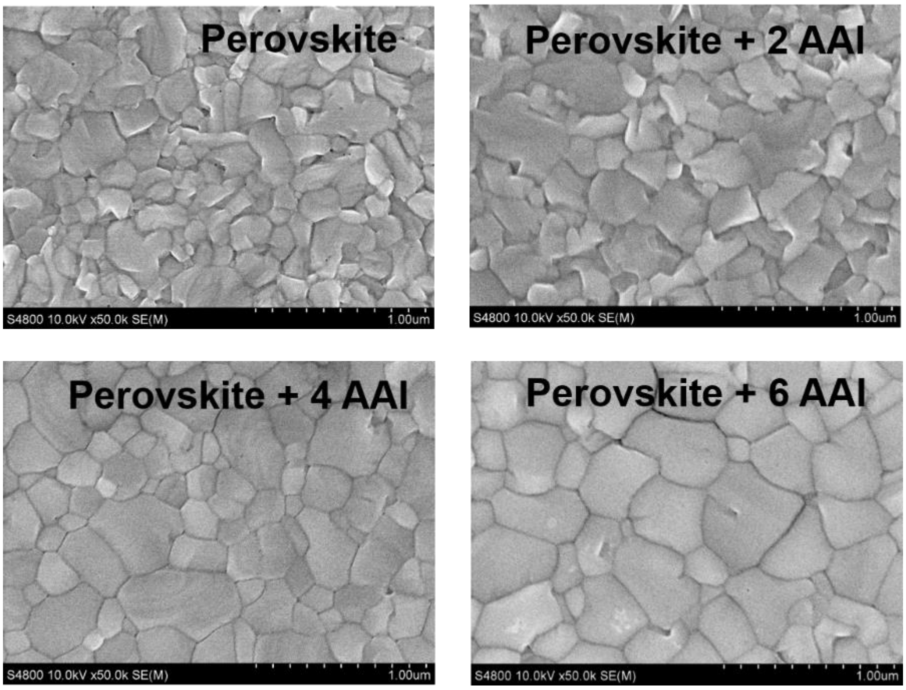

Fig. S9: SEM images of Pure Perovskite, and Perovskite mixed with 2-AAI, 4-AAI, and 6-AAI, derivatives respectively.

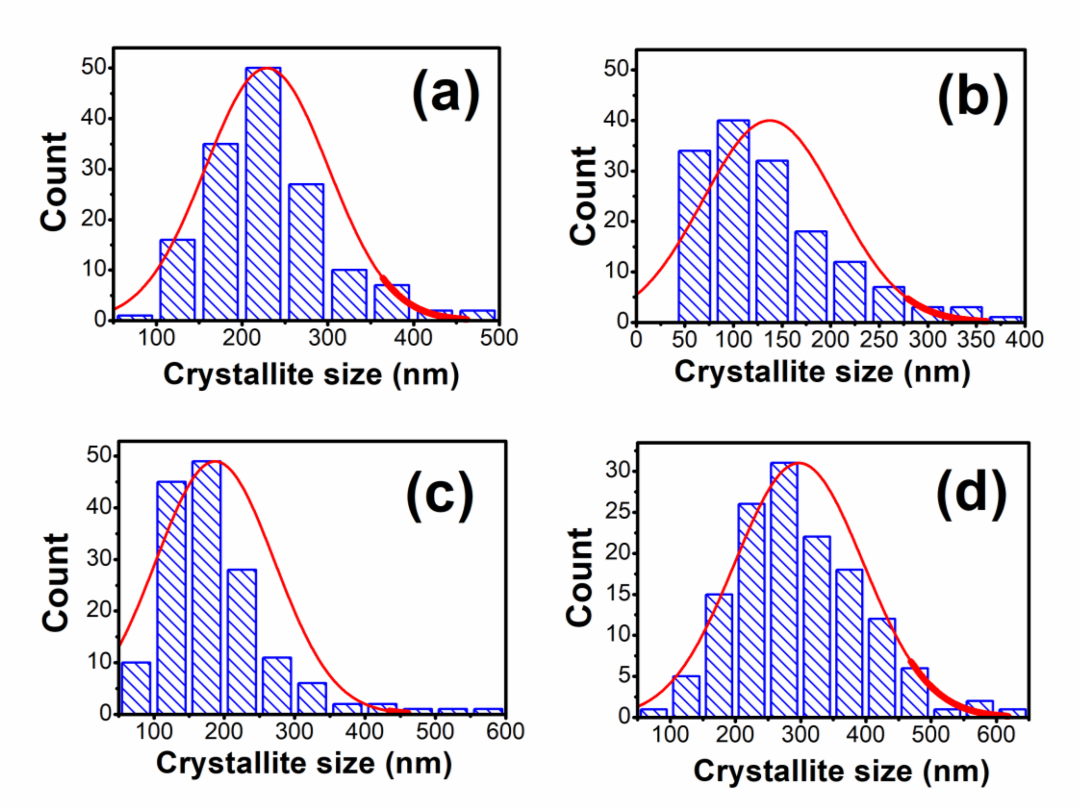

Fig. S10: Crystallite size distribution of (a) Pure Perovskite film, and Perovskite film mixed with (b) 2-AAI, (c) 4-AAI, and (d) 6-AAI, derivatives.